Real-time sampling electronics for double modulation experiments with Fourier transform infrared spectrometers

Michael J. Green, Barbara J. Barner, and Robert M. Corn[a)]
Department of Chemistry, University of Wisconsin, 1101 University Ave., Madison, Wisconsin 53706

(Received 17 December 1990; accepted for publication 13 February 1991)

A novel synchronous real-time analog sampling method for obtaining the sum and difference interferograms in double modulation Fourier transform infrared absorption experiments is described, and the application of this sampling methodology to polarization-modulation FTIR measurements of thin films at metal surfaces is demonstrated. A quadratic approximation of the background signal is used to calculate the difference interferogram. The demodulation of a test waveform with the real-time sampling electronics reveals how the bandwidth limitations of previous double modulation experiments on FTIR interferometers that employed lock-in amplifiers have been eliminated.

I. INTRODUCTION

Double modulation spectroscopy is a general method for obtaining the differential absorption spectrum of a sample. For example, infrared reflection-absorption spectroscopy (IRRAS) of molecules adsorbed onto metal surfaces has been performed with the polarization modulation experiment schematically depicted in Fig. 1.[1-7] In the traditional double modulation scanning experiments [Fig. 1(a)] the polarization of the light incident on a sample is modulated at a frequency ω_1 between p-polarized light (light polarized parallel to the plane of incidence) and s-polarized light (light polarized perpendicular to the plane of incidence) with a photoelastic modulator (PEM)[8] to obtain the differential reflectance spectrum, $\Delta R/R$:

$$\frac{\Delta R}{R}=\frac{I_p-I_s}{I_p+I_s}, \tag{1}$$

where I_p is the infrared spectrum obtained with p-polarized light and I_s the infrared spectrum obtained with s-polarized light. Since only p-polarized light has an appreciable amplitude at the metal surface (for a high angle of incidence),[9] the differential reflectance spectrum provides a direct measurement of the vibrational spectrum of the adsorbed molecules without the need for a background reference. In a scanning experiment,[1] the intensity of the source is modulated by a chopper at frequency ω_2 simultaneously with the modulation of the polarization at ω_1 to eliminate any background radiation. The polarization modulation frequency is typically 74 kHz, while the chopper frequency is typically $\leqslant 1$ kHz. As long as these two frequencies are well-separated, lock-in amplifiers referenced to ω_1 and ω_2 can be used to measure $(I_p - I_s)$ and $(I_p + I_s)$ very accurately and the differential reflectance spectrum can be obtained as a function of wavelength as the monochromator is scanned.

In polarization-modulation Fourier transform infrared reflection-absorption (PM-FTIRRAS) measurements[2-7] [Fig. 1(b)] this separation of frequencies is much more difficult. The spectral information of the interferometric experiment is contained in a bandwidth of frequencies typically ranging from several hundred to 20 kHz, and the polarization modulation spectrum is centered about 74 kHz. The resultant waveform is the sum of an average

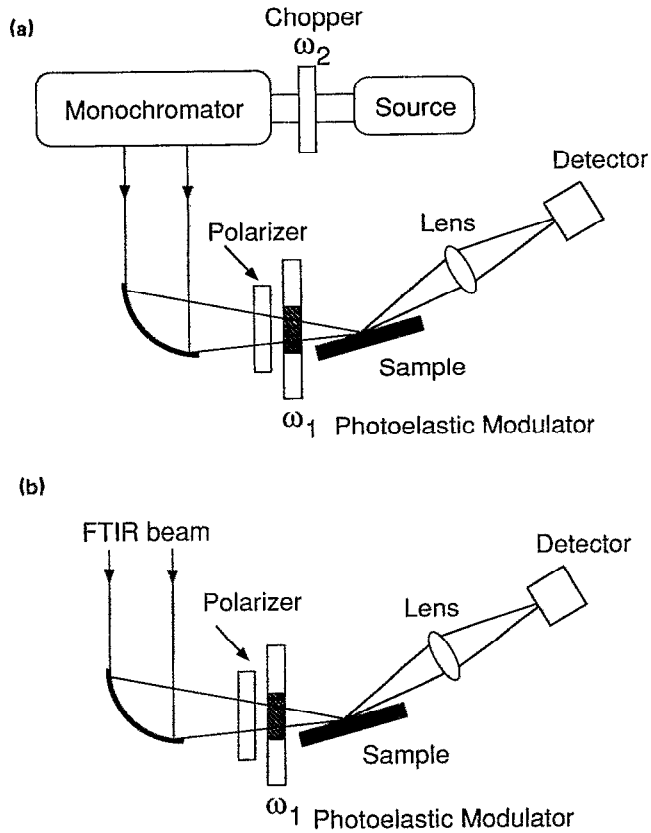

FIG. 1. Optical layout for polarization-modulation differential reflectance measurements. (a) Double modulation experiment using a scanning monochromator and photoelastic modulator to modulate the polarization at frequency ω_1. (b) PM-FTIRRAS experimental layout.

a)Author to whom correspondence should be addressed.

 0034-6748/91/061426-05$02.00

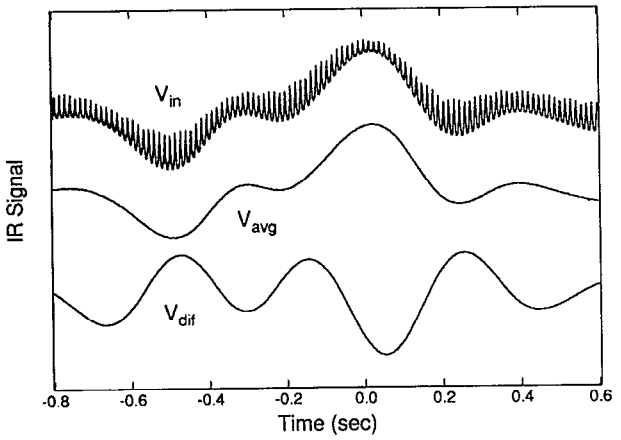

FIG. 2. PM-FTIRRAS interferogram from a 20 nm polyimide thin film on a chromium-coated silicon wafer. V_{in} is the PM-FTIRRAS interferogram, and V_{avg} and V_{dif} are the average and difference interferograms produced by the demodulation electronics. These two waveforms are digitized, transformed, and then ratioed to obtain the PM-FTIRRAS differential reflectance spectrum.

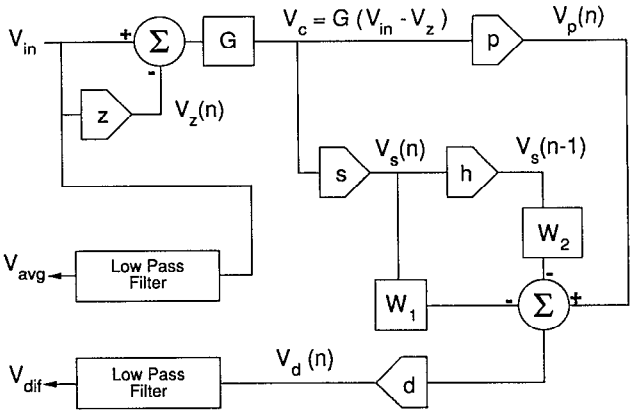

FIG. 3. Block diagram for the demodulation electronics. The circuit converts a double modulation waveform V_{in} into the average and difference waveforms V_{avg} and V_{dif}. Pentagons represent the synchronous sample-and-hold amplifiers, and are labeled according to when they are sampled during each modulation cycle. Squares in the diagram refer to gain or attenuation elements, and circles with the enclosed "Σ" refer to sum/difference amplifiers. The sign for each incoming signal to a sum/difference amplifier is shown at the inputs. Both V_{avg} and V_{dif} are sent through low pass filters to suppress any spurious high frequency modulation that is generated in the sampling process.

interferogram signal plus an additional modulation due to the PEM with an amplitude that is a function of mirror position. For example, the central region of a PM-FTIRRAS interferogram from a Cr-coated Si wafer with a thin (20 nm) film of polyimide is shown in Fig. 2. The polarization modulation of the interferogram at a frequency of 74 kHz is readily observable on the infrared signal. Most commercial lock-in amplifiers have a minimum time constant of about 0.5 ms and are thus unable to follow the rapid variations of the modulation amplitude in this experiment. To avoid this problem, the moving mirror of the infrared interferometer is usually slowed down to lower the bandwidth characteristics of the average interferogram to below 2 kHz, permitting the use of a lock-in amplifier.[2] This article describes a synchronous sampling method that we have recently implemented to obtain the differential reflectance spectrum from the polarization-modulated interferogram at normal mirror velocities.[7] The method samples the input waveform (V_{in}) three times during each PEM modulation cycle to obtain an average (V_{avg}) and a difference (V_{dif}) interferogram that can be transformed and then ratioed to obtain the differential reflectance spectrum.

II. EXPERIMENTAL CONSIDERATIONS

The interferogram and FTIR spectrum shown in this article were obtained with a Mattson Cygnus 100 FTIR spectrometer at a nominal resolution of 2 cm^{-1}. Polarization modulation of the infrared beam was obtained at a frequency of 74 kHz with a Hinds ZnSe photoelastic modulator. Further details of the optical components, the interface of the electronics to the spectrometer, and the preparation of the polyimide thin film sample have been given previously.[7] All voltage waveforms were obtained with a 125 MHz digital oscilloscope (LeCroy Model 9400).

III. METHODOLOGY

Figures 3 and 4 show a block diagram and timing scheme for the demodulator circuit that produces V_{avg} and V_{dif} from V_{in}. The circuit consists of five high quality (Crystal CS3112) video sample and hold amplifiers (pen-

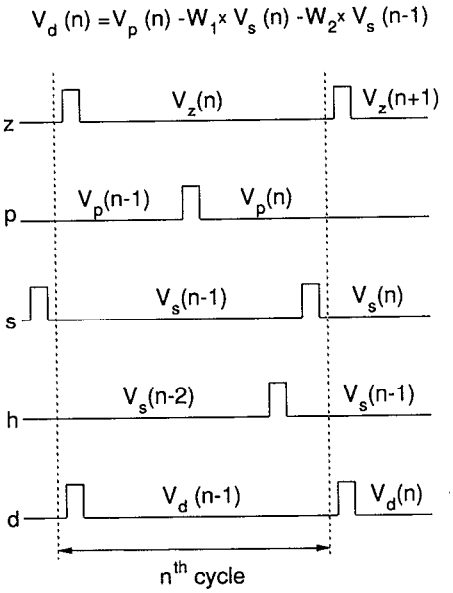

FIG. 4. Timing scheme for the demodulation electronics during the nth cycle. At the start of the cycle V_{in} is sampled to produce $V_z(n)$. These two signals are subtracted and amplified to produce the corrected signal V_c which is sampled at $V_p(n)$ and $V_s(n)$. Just prior to sampling $V_s(n)$ the voltage sampled at the end of the previous cycle $V_s(n-1)$ is sampled by circuit "h." Immediately after obtaining $V_s(n)$, the estimated modulation peak amplitude $V_d(n)$ is obtained from $V_p(n)$, $V_s(n)$, and $V_s(n-1)$.

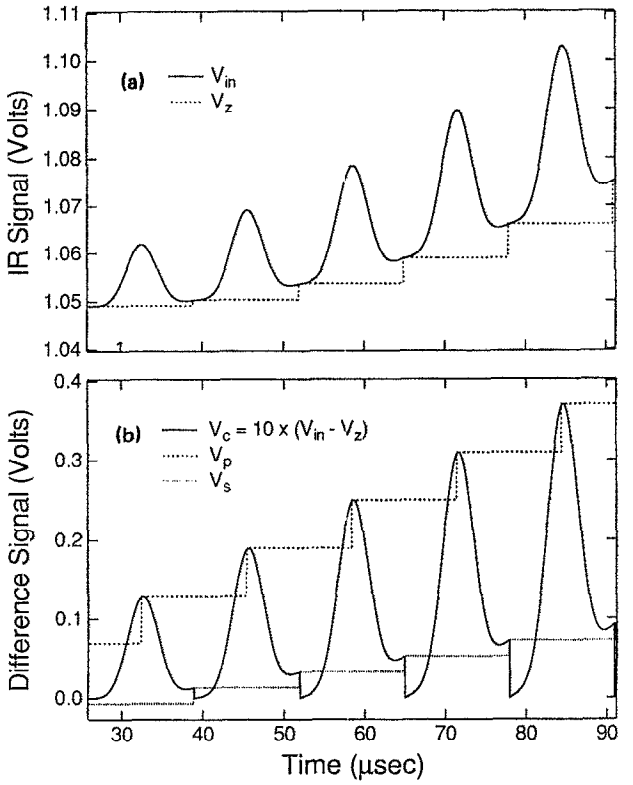

FIG. 5. Five cycles of a simulated PM-FTIRRAS signal. (a) Input voltage V_{in} and the sampled voltage V_z. (b) Corrected signal V_c and the sampled voltages V_p and V_s.

tagons), two summing amplifiers (circles), three gain/attenuation stages (squares) and two matched low-pass output filters. A TTL-level square wave reference output from the photoelastic modulator defines the cycle period for the synchronous sampling measurements; the five sample and hold circuits make measurements at fixed times during each modulation cycle (Fig. 4).

To describe the operation of the circuitry, five cycles of a simulated PM-FTIRRAS signal are shown in Fig. 5. At the beginning of each modulation cycle a voltage measurement of V_{in} is obtained with a sample and hold amplifier [Fig. 5(a)]. This voltage, V_z, is an approximation of the interferogram that would be obtained in the absence of polarization modulation, V_{bkg}, and is subtracted from the input voltage V_{in} to create the corrected signal V_c:

$$V_c = G(V_{in} - V_z), \tag{2}$$

where G is a gain factor that amplifies the small polarization-induced modulation of the infrared signal. This corrected signal for the simulated infrared waveform is shown in Figs. 5(b) and 6; in the current implementation of the electronics the gain is set to ten. Amplification of this signal allows the full dynamic range of the electronic circuitry to be utilized for the modulation measurement, and avoids potential degradation caused by further analog processing. The synchronous sampling electronics measures V_c with sample and hold circuits twice during each modulation cycle: once at the end of the cycle (V_s) and once at a set

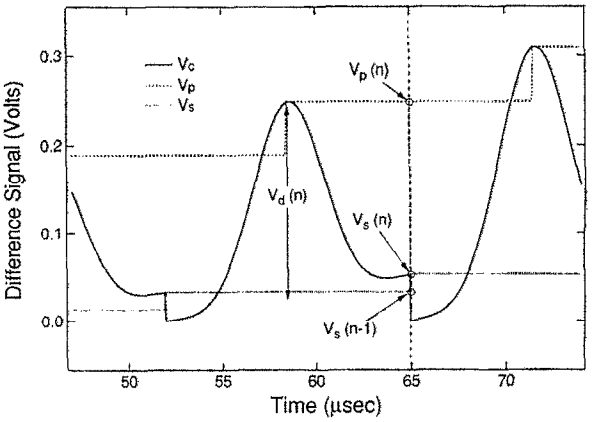

FIG. 6. Estimate of the modulation peak amplitude $V_d(n)$. $V_d(n)$ is obtained at the end of the modulation cycle from the three voltages $V_p(n)$, $V_s(n)$, and $V_s(n-1)$.

time during the modulation cycle at which the peak modulation signal occurs (V_p). The time at which V_p is measured is the same for each cycle, and is adjusted at the beginning of an experiment after an examination of the corrected signal on an oscilloscope.

At the end of each PEM cycle an estimate of the modulation amplitude, V_d, is made. For the nth cycle, the estimate $V_d(n)$ is obtained from three sampled voltages: $V_p(n)$, $V_s(n)$, and $V_s(n-1)$ (see Fig. 6). This last voltage, $V_s(n-1)$, is the voltage obtained at the end of the previous cycle, and is held in an additional sample and hold circuit "h" as shown in the block diagram and timing scheme (Figs. 3 and 4). Just prior to the acquisition of $V_s(n)$, the voltage held from the previous cycle, $V_s(n-1)$, is transferred to circuit "h."

Fractions of the two voltages $V_s(n)$ and $V_s(n-1)$ are subtracted from $V_p(n)$ in order to provide a better estimate of $V_d(n)$:

$$V_d(n) = V_p(n) - W_1 V_s(n) - W_2 V_s(n-1), \tag{3}$$

where W_1 and W_2 are the weighting factors. As seen in Fig. 6, if $V_p(n)$ alone were used as an estimate of the modulation amplitude (i.e.; if only the subtraction V_z from V_{in} were considered), the background correction would be incorrectly approximated. This is because V_{bkg}, the interferogram in the absence of polarization modulation, has changed from the time $V_z(n)$ was obtained to the time when $V_p(n)$ was acquired. If t_z is defined as the time at the beginning of the modulation cycle, t_p as the time during the modulation cycle when $V_p(n)$ is obtained, and t_s as the time at the end of the modulation cycle when $V_s(n)$ is acquired, then the value of the background at time t_p can be estimated from V_z at time t_z by a series expansion:

$$V_{bkg}(t_p) \approx V_{bkg}(t_z) + V'_{bkg}(t_z)\Delta t_p + V''_{bkg}(t_z)(\Delta t_p)^2/2 + \ldots, \tag{4}$$

where $\Delta t_p = t_p - t_z$, and $V'_{bkg}(t_z)$ and $V''_{bkg}(t_z)$ are the first and second derivatives of V_{bkg} evaluated at t_z. For the nth

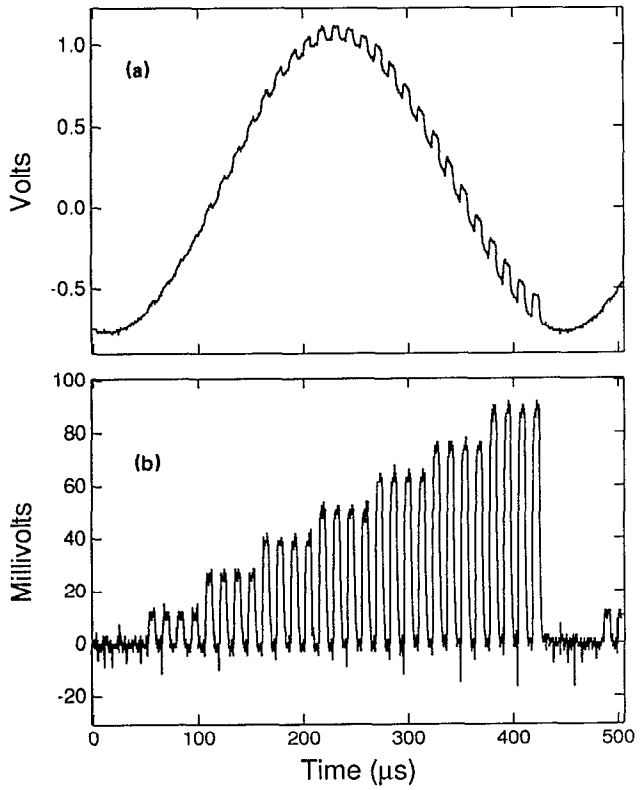

FIG. 7. Test double modulation waveform for the real-time sampling electronics. (a) Combination waveform with 2 kHz sine wave background and a small amplitude "stepped" modulation. (b) The test stepped modulation waveform without the background.

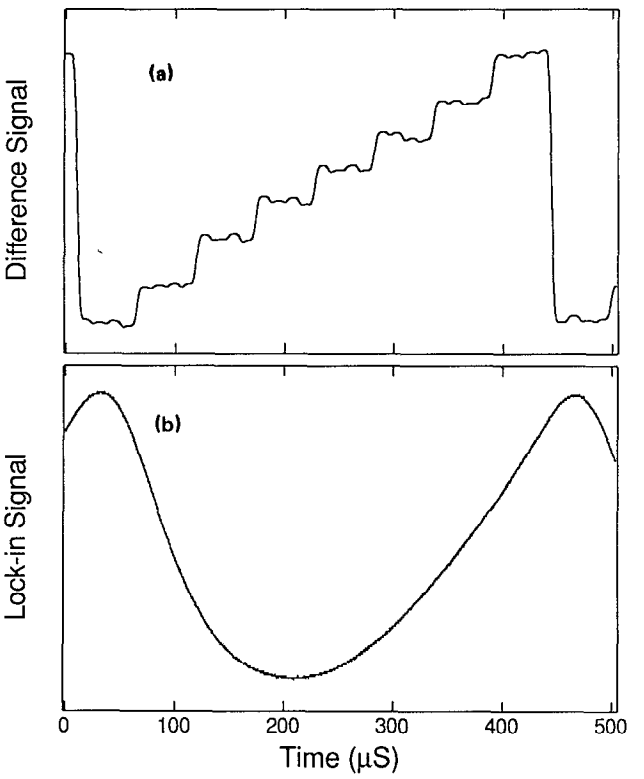

FIG. 8. Demodulation electronics and Lock-in amplifier performance test comparison. (a) Demodulation electronics output V_{dif} from the test double modulation waveform. (b) Lock-in amplifier response to the test double modulation waveform.

cycle, the measurement of V_{bkg} at t_z is $V_z(n)$, and the two derivatives can be approximated by:

$$V'_{\text{bkg}}(t_z) \approx \frac{[V_s(n) + V_s(n-1)]}{2G\Delta t_s}, \tag{5}$$

$$V''_{\text{bkg}}(t_z) \approx \frac{[V_s(n) - V_s(n-1)]}{G\Delta t_s^2}, \tag{6}$$

where $\Delta t_s = t_s - t_z$. From Eqs. (5) and (6) it can be shown that in order to correctly estimate the background to second order the weighting factors must be given by:

$$W_1 = \frac{1}{2}\left(\frac{\Delta t_p}{\Delta t_s} + \frac{\Delta t_p^2}{\Delta t_s^2}\right), \tag{7}$$

$$W_2 = \frac{1}{2}\left(\frac{\Delta t_p}{\Delta t_s} - \frac{\Delta t_p^2}{\Delta t_s^2}\right). \tag{8}$$

For example, if the peak measurement is made exactly in the middle of the modulation cycle, then $W_1 = 0.375$ and $W_2 = 0.125$. For the polarization-modulation interferograms used in the differential reflection-absorption measurements a quadratic background correction was sufficient to eliminate any leakage of the background voltage V_{bkg} into the difference signal waveform. Higher order corrections could have been added onto $V_d(n)$ by using additional sample and hold circuits to store more previous measurements of V_s. Because the calculation of $V_d(n)$ requires the voltage $V_s(n)$ acquired at t_s, the difference signal V_{dif} will be delayed in time by half a modulation cycle from when it occurs at t_p.

The difference signal V_{dif} is created from the voltage waveform V_d by filtering to remove any high frequencies introduced in the sampling. Concurrently the input voltage V_{in} is filtered in a similar fashion to obtain the average voltage signal V_{avg}. Both signals are sent to FTIR spectrometer where they are digitized, transformed, and then ratioed to obtain the differential reflection-absorption spectrum.[7]

IV. DEMODULATION PERFORMANCE TEST

To facilitate development and evaluation of the detection electronics, a double modulation test waveform generator was designed and constructed. The test waveform consisted of a 74 kHz pulse amplitude modulated signal superimposed upon a large 2 kHz sine wave background [Fig. 7(a)]. The 74 kHz modulation consisted of a repeated series of eight four-pulse sequences, each with a slightly larger amplitude [Fig. 7(b)]. Figure 8(a) plots the output signal V_{dif} obtained by the real-time sampling electronics from the test waveform. Virtually no sine wave background appears in the difference signal. For comparison, Fig. 8(b) shows the response of an E.G.&G. Model 124A lock-in amplifier to the same input signal. Even though the lock-in was operated with it minimum output time constant, it is apparent from the figure that the lock-in is un-

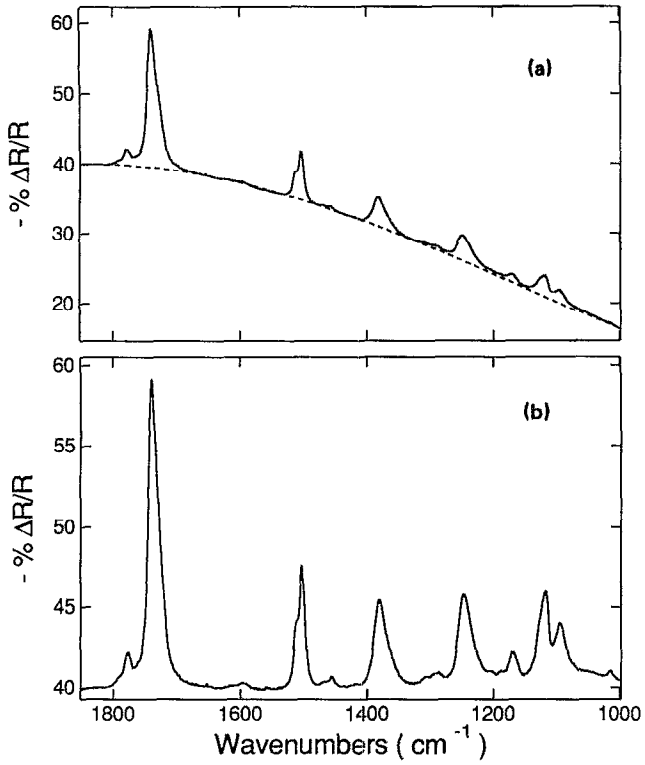

FIG. 9. PM-FTIRRAS differential reflectance spectrum of a 20 nm polyimide thin film on a Cr-coated silicon wafer. (a) Differential reflectance spectrum obtained after transforming and ratioing V_{dif} and V_{avg} from an experiment with the PEM set for polarization modulation at 1818 cm^{-1}. (b) Differential reflectance spectrum after normalization for the wavelength dependence of the PEM modulation efficiency. Reprinted with permission from Ref. 7 (copyright © 1990 by the American Chemical Society).

able to recover the stepped waveform, whereas the real-time sampling electronics faithfully reproduces the eight-step amplitude modulation signal.

V. APPLICATION TO POLARIZATION MODULATION-FTIR EXPERIMENTS

The application of the real-time sampling electronics to PM-FTIRRAS experiments results in the accurate measurement of the differential reflection-absorption spectrum. For example, processing the PM-FTIRRAS waveform shown in Fig. 2 with the real-time sampling electronics leads to the two signals V_{avg} and V_{dif} shown in the figure. These "sum" and "difference" interferograms are sent to the spectrometer, digitized, and transformed to obtain the sum and difference spectra $I_{avg}(\omega)$ and $I_{dif}(\omega)$, respectively. The ratio I_{dif}/I_{avg} yields the differential reflectance spectrum $\Delta R/R$ times a weighting term that results from the variation of the PEM modulation efficiency as a function of wavelength.[7] Figure 9(a) plots the ratio I_{dif}/I_{avg} for a PM-FTIRRAS experiment where the PEM was nominally set for most efficient modulation at 5.50 μm (1818 cm^{-1}). Normalization of the ratio by this weighting term results in the spectrum shown in Fig. 9(b). In a previous paper, it was demonstrated that the real-time sampling electronics can provide sufficient sensitivity to obtain the differential reflectance spectrum from monolayers at metal surfaces.[7] Note in Fig. 9 the absence of any residual atmospheric water bands due to the lack of preferential absorption for *s*-polarized or *p*-polarized light by the water molecules. This insensitivity to molecules that are not near the surface has led to the application of PM-FTIRRAS measurements for *in situ* measurements in thin film electrochemical cells.[6]

In addition to metal surfaces, the demodulation electronics described in this paper can in principle be applied to a variety of PM-FTIRRAS measurements. For example, infrared vibrational circular dichroism measurements[10] result in a similar modulated interferogram, and the synchronous sampling electronics could be applied directly to such systems. Other double modulation FTIR experiments to which the real-time sampling electronics could be applied are linear dichroism in stretched polymer films,[11] photodeflection measurements,[12] and attenuated total reflection (ATR) geometries.[13]

ACKNOWLEDGMENTS

This work was supported by grants from the National Science Foundation and the Wisconsin Alumni Research Foundation (WARF).

[1] (a) W. G. Golden, D. S. Dunn, and J. Overend, J. Catal. **71**, 395 (1981); (b) W. G. Golden, D. D. Saperstein, M. W. Severson, and J. Overend, J. Phys. Chem. **88**, 572 (1984).
[2] W. G. Golden, Fourier Transform Infrared Spectrosc. **4**, 315 (1985).
[3] A. E. Dowry and C. Marcott, Appl. Spectrosc. **36**, 414 (1982).
[4] W. G. Golden and D. D. Saperstein, J. Electron Spectrosc. Relat. Phenom. **30**, 43 (1983).
[5] T. Buffeteau, B. Desbat, and J. M. Turlet, Mikrochim. Acta [Wien] II, 23 (1988).
[6] (a) W. G. Golden, K. Kunimatsu, and H. Seki, J. Phys. Chem. **88**, 1275 (1984); (b) K. Kunimatsu, W. G. Golden, H. Seki, and M. R. Philpott, Langmuir **1**, 245 (1985).
[7] B. J. Barner, M. J. Green, E. I. Saez, and R. M. Corn, Anal. Chem. **63**, 55 (1991).
[8] K. W. Hipps and G. A. Crosby, J. Phys. Chem. **83**, 555 (1979).
[9] (a) R. G. Greenler, J. Chem. Phys. **44**, 310 (1966); (b) R. G. Greenler, J. Chem. Phys. **50**, 1963 (1969).
[10] (a) L. A. Nafie and M. Diem, Appl. Spectrosc. **33**, 130 (1979); (b) L. A. Nafie and D. W. Vidrine, Fourier Transform Infrared Spectrosc. **3**, 83 (1982).
[11] I. Noda, A. E. Dowry, and C. Marcott, Appl. Spectrosc. **42**, 203 (1988).
[12] A. L. Crumbliss, P. S. Lugg, J. W. Childers, and R. A. Palmer, J. Phys. Chem. **89**, 482 (1985).
[13] (a) H. Neff, P. Lange, D. K. Roe, and J. K. Sass, J. Electroanal. Chem. **150**, 513 (1983); (b) N. J. Harrick, J. Phys. Chem. **83**, 555 (1960).